Isopropanol oxidation by pure metal oxide catalysts: number of active surface sites and turnover frequencies

Deepak Kulkarni, Israel E. Wachs[*]

Department of Chemical Engineering, Zettlemoyer Center for Surface Studies, Lehigh University, Bethlehem, PA 18015, USA

Abstract

The objective of the present study was to determine the number of active surface sites and their nature, redox or acidic, for bulk metal oxide catalysts using isopropanol as a chemical probe molecule. Isopropanol oxidation activity on the following metal oxides was investigated: MgO, CaO, SrO, BaO, Y_2O_3, La_2O_3, CeO_2, TiO_2, ZrO_2, HfO_2, V_2O_5, Nb_2O_5, Ta_2O_5, Cr_2O_3, MoO_3, WO_3, Mn_2O_3, Fe_2O_3, Co_3O_4, Rh_2O_3, NiO, PdO, PtO, CuO, Ag_2O, Au_2O_3, ZnO, Al_2O_3, Ga_2O_3, In_2O_3, SiO_2, SnO_2 and Bi_2O_3. On average, the number of active surface sites for isopropanol dissociative adsorption on these catalysts was $\sim$2–4 μmol/m^2. The number of active surface sites enabled quantification of the turnover frequency (TOF) for these catalysts. The TOF values for the various pure metal oxides were normalized at 200 °C. The TOFs of catalysts showing redox activity vary by six-orders of magnitude (10^2 to 10^{-4} s^{-1}). For catalyst showing acidic activity, the TOFs varied by over eight-orders of magnitude (10^1 to 10^{-7} s^{-1}). The reaction products from isopropanol oxidation at low conversions reflected the nature of the active surface sites, redox or acidic, on these catalysts. Redox surface sites yield acetone and acidic surface sites yield propylene. Small amounts of isopropyl ether formation are sometimes also observed via bimolecular recombination of surface isopropoxide species on acidic surface sites. All catalysts with the exception of Fe_2O_3 and TiO_2, exhibited extremely high selectivity to either redox or acidic products. Except for the sharp decrease in TOFs towards redox products with increasing bulk M–O heats of formation at low $-\Delta H_f$, no correlations were found between the TOFs and bulk metal oxide properties (TPR–H_2 and $-\Delta H_f$). However, an inverse relation was found between the TOFs (redox) and the surface isopropoxide intermediate decomposition temperature at low decomposition temperatures. At moderate and high decomposition temperatures, the TOFs (redox) were almost independent of the surface isopropoxide decomposition temperature. The selectivity of the metal oxide catalysts was found to be independent of the TOFs.
© 2002 Elsevier Science B.V. All rights reserved.

1. Introduction

The intrinsic catalytic activity of different metal oxide catalysts can best be compared when expressed by their turnover frequency (TOF = molecules converted per active surface site per second) [1]. To determine the TOF, it is necessary to quantify the number of active surface sites on the metal oxide catalyst. Several approaches have been proposed to quantify the active surface sites. One common approach is O_2 chemisorption [2–10], which involves reducing the catalyst surface with H_2 and reoxidation to determine the number of active surface sites by the amount of O_2 adsorbed. This is not a very accurate method since over

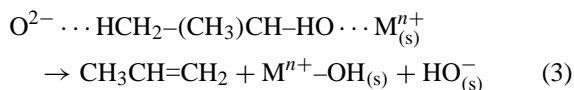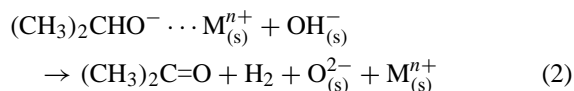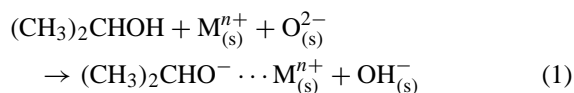* Corresponding author. Tel.: +1-610-758-4274;
fax: +1-610-758-6555.
E-mail address: iew0@lehigh.edu (I.E. Wachs).

reduction of the metal oxide surface can usually take place. Other methods involve the adsorption of CO_2 and NH_3. CO_2 and NH_3 do not measure all the surface sites. CO_2 only adsorbs on basic OH groups on the surface and NH_3 only adsorbs on Lewis and Bronsted acid sites. Furthermore, the above methods are unable to distinguish between surface acidic and redox sites.

The adsorption and reaction of alcohols on metal oxide catalysts has been used as a chemical probe reaction for many years. Alcohol reactions have been studied extensively using temperature programmed decomposition (TPD), steady-state kinetic studies, in situ spectroscopy, microcalorimetry and many ultra-high vacuum surface science studies as cited by Rekoske and Barteau [11]. Isopropanol decomposition has long been considered as a chemical probe reaction for surface acid–base properties [12]. Isopropanol undergoes dehydration to give propylene on acidic surface sites and dehydrogenation via a concerted mechanism on adjacent acidic and basic surface sites to give acetone. Ai and Suzuki were the first to correlate various acidic and basic properties of metal oxide catalysts with their rates of dehydration and dehydrogenation of isopropanol [12]. Similar to methanol and ethanol, isopropanol also undergoes a bimolecular reaction caused by the coupling of two surface isopropoxide species to give isopropyl ether on acidic surface sites. However, formation of ether is minimized in the presence of oxygen according to previous studies [11]. The oxidation and decomposition reactions are analogous, since the only role of oxygen is to prevent the reduction of the metal oxide surface. The partial oxidation of alcohols on TiO_2, CuO and Co_3O_4 follows a Mars–van Krevelen mechanism, i.e. zero-order with respect to oxygen, which suggests that lattice oxygen, rather than gas phase oxygen, is directly involved in metal oxide catalysts [11,13,14]. Decomposition studies have indicated that at sufficiently high partial pressures of isopropanol the reaction rate also becomes pseudo zero-order with respect to isopropanol [15]. On niobium oxide, Ouquor et al. found the reaction to be zero-order with respect to isopropanol when the partial pressure of isopropanol exceeded 2 kPa [15].

The chemisorption and reaction of isopropanol on some metal oxides have been extensively studied. One of the most commonly studied oxides is TiO_2 [11,16–20]. Isopropanol adsorption has also been employed as a method of measuring the surface titania

content in mixed titania-silica catalysts [21,22]. Zaki and coworkers have done in situ IR spectroscopy studies of isopropanol adsorption on Al_2O_3, CeO_2, TiO_2, ZrO_2 and HfO_2 [23,24]. Other metal oxides that have been extensively studied are ZnO [25,26] and MoO_3 [27]. All these investigations adsorbed isopropanol at room temperature and found that isopropanol adsorbs both dissociatively as a surface isopropoxide intermediate and as physisorbed isopropanol at room temperature. In some cases, also intact isopropanol was chemisorbed via coordinative bonding to the metal oxide surface. This coordinatively bonded isopropanol was also found on Y_2O_3 at up to 250 °C [28]. Upon evacuation most of the physisorbed isopropanol desorbed leaving only the surface isopropoxide species and the coordinatively bonded isopropanol. Dehydroxylated surfaces dissociated isopropanol to give isopropoxide species and surface hydroxyls. The hydroxyl species desorbed as water upon heating to sufficiently high temperatures. The surface isopropoxide species underwent further C–H bond scission at higher temperatures to give acetone. Two kinds of surface isopropoxide species were observed on metal oxide catalysts. One of the surface alkoxides is terminally bonded to a single cation and the other is bridge bonded to two cations. Hussein and Gates [28] propose that the bridge bonded species yield propylene and the terminal species give acetone. The surface reactions to the acetone and propylene are shown below:

$$(CH_3)_2CHOH + M^{n+}_{(s)} + O^{2-}_{(s)}$$
$$\rightarrow (CH_3)_2CHO^- \cdots M^{n+}_{(s)} + OH^-_{(s)} \quad (1)$$

$$(CH_3)_2CHO^- \cdots M^{n+}_{(s)} + OH^-_{(s)}$$
$$\rightarrow (CH_3)_2C{=}O + H_2 + O^{2-}_{(s)} + M^{n+}_{(s)} \quad (2)$$

$$O^{2-} \cdots HCH_2{-}(CH_3)CH{-}HO \cdots M^{n+}_{(s)}$$
$$\rightarrow CH_3CH{=}CH_2 + M^{n+}{-}OH_{(s)} + HO^-_{(s)} \quad (3)$$

where M^{n+} is the positive metal cation to which the surface isopropoxide species are bonded.

One of the objectives of the present investigation is to determine the number of active surface sites per m^2 (N_s) and also the isopropanol oxidation turnover frequencies on the various metal oxide catalysts. Isopropanol can distinguish between acidic and redox surface sites as discussed above, unlike most other

common probe molecules such as O_2, CO and H_2. Isopropanol was adsorbed on the metal oxides at an elevated temperature of $110\,^{\circ}$C in order to minimize the physically adsorbed isopropanol. Methanol chemisorption studies have shown that the physisorbed methanol desorbs $<100\,^{\circ}$C [29,30]. On alumina it was observed that the hydrogen bonded alcohol molecules are partially desorbed by $100\,^{\circ}$C and completely desorbed along with the decomposition of surface alkoxide species at $200\,^{\circ}$C [23].

Another objective of the study was to determine the isopropanol oxidation activity and selectivity of the various metal oxide catalysts as well as their apparent activation energies towards the different reaction products. The number of active surface sites data along with oxidation reactivity data allows quantitative determination of the TOFs of the pure metal oxide catalysts, and comparison of their inherent catalytic properties.

Temperature programmed decomposition (TPD) was used to determine the decomposition temperature of the surface isopropoxide species from the various metal oxide surfaces. The scission of the C–H bond on the α-carbon atom is known to be the rate-determining step in isopropanol reactions and, consequently, is an important parameter for fundamentally understanding the catalytic reaction characteristics [11,15].

2. Experimental

2.1. Catalyst synthesis

The bulk metal oxide catalysts used in the present study were purchased as high purity commercial oxides or oxides prepared by the decomposition of their corresponding hydroxides or metal salts as shown in Table 1. The pre-treatment conditions were obtained from the Handbook of Chemistry and Physics [31]. The purity of the commercial metal oxides is mentioned in Table 1 and that of the precursors is mentioned by Briand and Wachs [32].

2.2. Bet surface area

The BET surface area of each sample was determined by nitrogen adsorption/desorption isotherms on a Quantasorb surface area analyzer (Quantachrome

Table 1
Preparation of bulk metal oxide catalysts

Oxide catalyst	Method of preparation
MgO	$MgCO_3$, calcined at $350\,^{\circ}$C for 3 h, Aldrich
CaO	$CaCO_3$, calcined at $350\,^{\circ}$C for 3 h, Aldrich
BaO	$Ba(ClO_4)_2 \cdot 3H_2O$, calcined at $400\,^{\circ}$C for 3 h, Aldrich
Y_2O_3	Alfa Aesar, 99.999%
La_2O_3	Alfa Aesar, 99.999%
TiO_2	Degussa P-25
ZrO_2	Degussa
HfO_2	Alfa Aesar, 99.9%
CeO_2	Engelhard
V_2O_5	NH_4VO_3, calcined at $450\,^{\circ}$C for 3 h, Alfa Aesar
Nb_2O_5	Niobium Products Company
Ta_2O_5	H.C. Starck Company
Cr_2O_3	Alfa Aesar, 99.997%
MoO_3	$(NH_4)Mo_7O_{24} \cdot 4H_2O$ at $300\,^{\circ}$C for 5 h, Alfa Aesar
WO_3	H_2WO_4, calcined at $400\,^{\circ}$C for 48 h, Aldrich
Mn_2O_3	$Mn(OOCCH_3)_2$, calcined at $250\,^{\circ}$C, overnight, Alfa Aesar
Fe_2O_3	Alfa Aesar, 99.9%
CO_3O_4	Aldrich
Rh_2O_3	$Rh(NO_3)_2$, calcined at $300\,^{\circ}$C for 4 h, Johnson Mathey
NiO	$Ni(OH)_2$, calcined at $230\,^{\circ}$C, overnight, Alfa Aesar
PdO	$Pd(NO_3)_2$, calcined at $300\,^{\circ}$C for 4 h, Johnson Mathey
PtO	$Pt(NH_3)_4Cl_2$, calcined at $400\,^{\circ}$C for 4 h, Johnson Mathey
CuO	$Cu(NO_3)_2 \cdot 3H_2O$, calcined at $200\,^{\circ}$C for 48 h, Alfa Aesar
Ag_2O	Alfa Aesar, 99.9%
Au_2O_3	$Au(OH)_2$ calcined at $200\,^{\circ}$C for 48 h, Alfa Aesar
ZnO	Aldrich, 99.97%
Al_2O_3	Englehard
Ga_2O_3	Alfa Aesar, 99.999%
In_2O_3	Alfa Aesar, 99.997%
SiO_2	Cabosil EH-5
SnO_2	Aldrich, 99.97%
Bi_2O_3	$Bi_2(C_2O_4)_3$ at $300\,^{\circ}$C for 3 h, Aldrich

Corporation, Model OS-9) using a 3:7 ratio of N_2:He mixture. Typically, 0.2–0.3 g of sample was used for the measurement and the sample was outgassed at $250\,^{\circ}$C prior to N_2 adsorption.

2.3. XPS analysis

XPS analysis was performed on active metal oxides of IB group (Cu, Ag, Au) to determine the presence of

surface impurities. A Scienta model ESCA-300 X-ray photoelectron spectrometer was used for the analysis.

2.4. TPR–H_2

TPR–H_2 studies done on similar samples have been published previously [33]. The T_{onset} reduction value is plotted against the TOFs (redox) in Fig. 2.

2.5. Isopropanol chemisorption

The number of active surface sites for isopropanol chemisorpiton, were determined using a Cahn TGA microbalance (Model TG-131) coupled with a PC for temperature control, weight monitoring and data collection. A flow diagram of the set-up can be found in a prior publication [30]. The system allowed for a controlled flow of high purity gases: air during pre-treatment, a mixture of isopropanol and helium for adsorption phase and helium for the temperature programmed desorption phase. The following experimental procedure was employed. A weighed amount of catalyst was loaded into the TGA. The sample was initially heated to 350° for 1 h in flowing air (9.5 ml/min; ultra high purity; air gas) and helium (80 ml/min; ultra high purity; air gas) in order to remove adsorbed moisture and possible carbonaceous residues. The samples were then cooled to 110 °C in flowing helium (80 ml/min). Isopropanol was adsorbed on the catalyst from a stream of flowing $(CH_3)_2CHOH$ (2000 ppm)/He. The decomposition temperature of the surface decomposition species was determined by ramping up the temperature after isopropoxide adsorption at a constant rate of 10 °C/min until 500 °C and monitoring the derivative of the weight loss.

Adsorption at temperature <110 °C results in co-adsorption of physically adsorbed molecular isopropanol along with surface isopropoxide species. At temperatures significantly >110 °C, the surface isopropoxide species decomposed yielding reaction products. Therefore, 110 °C was chosen as the adsorption temperature since it minimized physisorption and optimized the dissociative chemisorption of isopropanol. A low isopropanol partial pressure (2000 ppm) was used in order to minimize the physically adsorbed isopropanol due to its condensation on catalyst pores. Adsorption on some very active metal oxides (PtO,

PdO, Ag_2O, Au_2O_3) catalysts was carried out at lower temperature (50 °C) due to the fact that the isopropoxide species decomposed at temperatures significantly <110 °C and that the precious metal catalysts have a tendency to reduce. Chemisorption was carried out on Fe_2O_3 and TiO_2 at 50 and 100 °C and the number of active surface sites for the active metal oxides was corrected to 110 °C.

2.6. Isopropanol oxidation

Isopropanol oxidation was used to determine catalytic reactivity and selectivity of the various metal oxides. The reaction was carried out in an isothermal fixed-bed differential reactor made of pyrex glass. The glass tube reactor had an inner diameter of 3.8 mm. Approximately 40 mg of the catalyst was tested for its isopropanol activity and selectivity at varying temperatures and at about atmospheric pressures (1.3 bar). The flow of oxygen and helium was controlled with two Brooks mass flow controllers (Brooks Model No. 5890 D). The gases were then passed through a saturator with isopropanol maintained at 8.6 °C. The ratio of the gases were found to be ~2:13:85 for $CH_3CH_2CHOH:O_2:He$, respectively. The reaction products and isopropanol conversion were determined by using an online gas chromatograph (HP 5890 Series II) equipped with TCD and FID detectors. A CP-sil 5CB column was connected to the FID and a Carboxene 1000 45/60 was connected in parallel to the TCD. Each catalyst was pretreated by heating in a mixture of He and O_2 at 350 °C for half an hour and then cooled in He/O_2 mixture to room temperature.

The reaction temperature was increased gradually in the range of 80 °C after initial activity was seen from a catalyst. The rate of formation of the different products was expressed as the catalytic activity ($\mu mol/m^2 s$). The selectivity was expressed in terms of mole fractions of product and was the ratio of the yield of specific product to that of the total isopropanol converted. The GC was calibrated with specific gas composition of 0.5% isopropanol, 0.1% each of acetone, isopropyl ether and propylene, with the balance helium (air gas). The relative molar responses were found to be 1.098 for acetone, 0.979 for propylene and 0.434 for isopropyl ether with the response to isopropyl alcohol taken as 1.

3. Results

3.1. BET surface area measurements and XPS analysis

The surface areas of the pure metal oxide catalysts are given in Table 2. The catalysts commonly used as supports show high surface areas (Al_2O_3, CeO_2, SiO_2, TiO_2, ZrO_2, Nb_2O_5). The commercially purchased catalysts had a low surface area with the exception of Fe_2O_3, Ga_2O_3 and Y_2O_3, which had comparatively high areas. Most of the active metal oxides (PtO, CuO, Ag_2O, Au_2O_3, V_2O_5) had low surface areas.

Table 2
BET surface area and $-\Delta H_f$ for metal oxide formation per oxygen atom

Oxide catalyst	Surface area (m^2/g)	$-\Delta H_f$ (298 K, kcal/mol)
MgO	23	143.8
CaO	20	151.7
BaO	2	133
Y_2O_3	17	152
La_2O_3	5	179.7
TiO_2	50	107
ZrO_2	39	128.3
HfO_2	2	135.5
CeO_2	33	130
V_2O_5	4	74.6
Nb_2O_5	55	100
Ta_2O_5	4	97.2
Cr_2O_3	21	89.7
MoO_3	3	60.1
WO_3	15	65.2
Mn_2O_3	9	76.5
Fe_2O_3	21	66.1
Co_3O_4	3	49
Rh_2O_3	11	22.7
NiO	43	58.4
PdO	17	20.4
PtO	2	10
CuO	1	38.5
Ag_2O	1	6.95
Au_2O_3	2	−3.66
ZnO	9	83.36
Al_2O_3	180	133.3
Ga_2O_3	18	86.6
In_2O_3	3	74
SiO_2	300	101.5
SnO_2	8	69
Bi_2O_3	4	45.7

Metal oxides of the IB group (CuO, Ag_2O, Au_2O_3) exhibited high activity. An XPS analysis was carried out to determine surface impurities. The XPS analysis of CuO revealed the surface to be primarily CuO with traces of C and N. The surface of Ag_2O was mostly Ag_2O with traces of C and Na. XPS analysis of the Au_2O_3 revealed the surface to be mostly Au_2O_3 with trace amounts of Au metal, Na, Cl and C. No traces of any other active metals like Pt or Pd were found in any of the oxides investigated. The high activity for isopropanol partial oxidation seen from IB metal oxides is entirely due to the metal oxide surface.

3.2. Isopropanol chemisorption and decomposition temperatures

On a dehydroxylated surface at 110 °C, the dissociative adsorption of isopropanol is the predominant process and results in the formation of surface isopropoxide species and surface hydroxyl species. The various metal oxide catalysts studied and the corresponding number of active surface sites are given in Table 3. The active surface site density for surface isopropoxide species on metal oxides (N_s) is expressed in $\mu mol/m^2$. This is calculated from the weight gain of the sample after adsorption of isopropanol for 1 h at 110 °C, which showed saturation of the weight gain. For every two molecules of isopropanol dissociatively adsorbed, one molecule of water leaves the surface [27]. Therefore, to calculate the μmol of isopropoxide species adsorbed, the weight gain in μg is divided by 51.

Chemisorption on a few metal oxides was carried out at a lower temperature, 50 °C, due to their higher reactivity, since these catalysts exhibited reactivity <110 °C (Au_2O_3, Ag_2O, PtO, PdO, Rh_2O_3). Also Ag_2O, Au_2O_3, PtO and CuO could become reduced at 110 °C. To ensure the accurate N_s measurements on these oxides the temperature has to be lowered. In order to account for the additional weight gained by the catalyst due to increase in physisorption at a lower temperature, a correction factor of 0.9 was obtained by comparing the adsorption of the Fe_2O_3 and TiO_2 at 110 and 50 °C, respectively. The corrected values are also shown in Table 3. It was observed that for chemisorption at temperatures slightly >110 °C, the amount of isopropanol adsorption did not vary significantly.

Table 3
Number of active surface sites on oxide catalyst

Oxide catalyst	No. of active sites (μmol/m^2)
MgO	8.9
CaO	2.7
BaO	0.7
Y_2O_3	3.1
La_2O_3	5.3
TiO_2	3.2
ZrO_2	2.6
HfO_2	3.1
CeO_2	2.5
V_2O_5	1.6
Nb_2O_5	2.0
Ta_2O_5	3.6
Cr_2O_3	0.7
MoO_3	1.2
WO_3	0.7
Mn_2O_3	2.6
Fe_2O_3	7.9
Co_3O_4	3.9
Rh_2O_3	2.7 (2.4)[a]
NiO	2.8
PdO	8.3 (7.5)[a]
PtO	2.1 (1.9)[a]
CuO	4.3 (3.9)[a]
Ag_2O	5.8 (5.2)[a]
Au_2O_3	36.5 (33)[a]
ZnO	1.7
Al_2O_3	2.8
Ga_2O_3	3.4
In_2O_3	2.0
SiO_2	0.5
SnO_2	2.1
Bi_2O_3	2.0

[a] Values corrected for adsorption at 110 °C.

Table 4
Surface isopropoxide decomposition temperature (T_d)

Oxide catalyst	Surface isopropoxide decompostion temperature (°C)
MgO	230
CaO	238
BaO	225
Y_2O_3	240
La_2O_3	328
TiO_2	265
ZrO_2	280
HfO_2	295
CeO_2	190
V_2O_5	170
Nb_2O_5	225
Ta_2O_5	272
Cr_2O_3	190
MoO_3	170
WO_3	200
Mn_2O_3	195
Fe_2O_3	231
Co_3O_4	203
Rh_2O_3	140
NiO	187
PdO	64
PtO	47
CuO	262
Ag_2O	83
Au_2O_3	49
ZnO	250
Al_2O_3	222
Ga_2O_3	210
In_2O_3	255
SiO_2	356
SnO_2	219
Bi_2O_3	230

The average active surface site density for isopropanol adsorption on metal oxide surface was found to be $\sim$2–4 μmol/m^2. Some of the active metal oxides possessed a higher active site density. Many of the basic metal oxides exhibited a lower value than would be expected from methanol chemisorption studies [33], since their surfaces have been dehydroxylated during the pre-treatment. SiO_2, Cr_2O_3, WO_3 and BaO show a somewhat lower active surface site density. SiO_2 is extremely unreactive and has a low N_s in spite of having a high surface area. The density of the active surface sites was reproducible within 0.3 μmol/m^2.

In order to determine the decomposition temperature of the surface isopropoxide species, a TPD experiment was also conducted after the isopropanol chemisorption experiment in the TGA apparatus. The surface isopropoxide decomposition temperatures on the various metal oxides are listed in Table 4.

Most of the catalysts showed an extremely high selectivity towards acetone or propylene. Consequently, it was possible to determine the decomposition temperature of the surface species that is most active. The decomposition temperatures of the surface isopropoxide intermediates are given in Table 4. PtO has the lowest isopropoxide decompostion temperature, $\sim$50 °C among pure redox catalysts compared to La_2O_3, whose decompostion temperature is in excess of 300 °C. In general the precious metal oxides had a low decomposition temperature ($\sim$50–120 °C). On the

other hand, most of the acidic catalysts had their decomposition temperature in the range of 150–300 °C. Most of the metal oxide catalysts had desorption peaks showing a normal distribution skewed slightly towards higher temperature. The peak width at half height was in the range of 25–40 °C for most catalysts. The peak widths at half height could not be determined for the very active precious metal oxides (PtO, Au$_2$O$_3$).

3.3. Steady-state isopropanol oxidation selectivity and TOF

The temperature range in which each of the metal oxides was tested for isopropanol oxidation is presented in Table 5. The selectivity to acetone, propylene

Table 5
Temperature range in which the catalysts were tested for isopropanol oxidation

Catalyst oxide	Temperature range (°C)
MgO	175–255
CaO	200–255
BaO	185–270
Y$_2$O$_3$	205–250
La$_2$O$_3$	260–300
TiO$_2$	235–300
ZrO$_2$	260–305
HfO$_2$	265–310
CeO$_2$	200
V$_2$O$_5$	135–190
Nb$_2$O$_5$	200–245
Ta$_2$O$_5$	230–290
Cr$_2$O$_3$	190–260
MoO$_3$	135–175
WO$_3$	175–210
Mn$_2$O$_3$	125–200
Fe$_2$O$_3$	160–245
Co$_3$O$_4$	200–240
Rh$_2$O$_3$	125–200
NiO	135–200
PdO	40–70
PtO	40–80
CuO	200–280
Ag$_2$O	100–125
Au$_2$O$_3$	40–60
ZnO	240–290
Al$_2$O$_3$	190–220
Ga$_2$O$_3$	190–217
In$_2$O$_3$	200–230
SiO$_2$	300–400
SnO$_2$	195–245
Bi$_2$O$_3$	195–285

Table 6
Isopropanol oxidation turnover frequencies (TOFs) at 200 °C

Catalyst oxide	TOF (s^{-1})	
	Redox	Acidic
MgO	0.004	–
CaO	0.0098	–
BaO	0.28	–
Y$_2$O$_3$	0.0098	–
La$_2$O$_3$	0.0097	–
TiO$_2$	0.00029	0.0002
ZrO$_2$	–	6.50E−07
HfO$_2$	–	0.00027
CeO$_2$	0.01	–
V$_2$O$_5$	0.018	18
Nb$_2$O$_5$	–	0.001
Ta$_2$O$_5$	–	0.0008
Cr$_2$O$_3$	0.054	–
MoO3	–	3.6
WO$_3$	–	0.21
Mn$_2$O$_3$	0.12	–
Fe$_2$O$_3$	0.023	0.011
Co$_3$O$_4$	0.031	–
Rh$_2$O$_3$	0.089	–
NiO	0.063	–
PdO	0.26	–
PtO	110	–
CuO	0.13	–
Ag$_2$O	0.75	–
Au$_2$O$_3$	29	–
ZnO	0.15	–
Al$_2$O$_3$	–	0.022
Ga$_2$O$_3$	–	0.031
In$_2$O$_3$	0.2	0.00044
SiO$_2$	–	0.0011
SnO$_2$	0.028	5.30E−05
Bi$_2$O$_3$	0.083	–

and diisopropyl ether production during isopropanol oxidation over the various metal oxide catalysts are presented in Table 6. The activities of the metal oxides to the acidic and redox products are extrapolated to 200 °C. The apparent activation energies for isopropanol oxidation over the metal oxide catalysts are presented in Table 7. It is observed that the apparent activation energy is not affected by variations in temperature and that the limitations due to mass and heat transfer are absent. With the help of these tables it is possible to calculate the activities of the catalysts to propylene and acetone under differential conversion conditions (<10%). Almost all the catalysts showed a small range of temperature (<80 °C) in which the

Table 7
Apparent activation energies for redox and acidic reactions during isopropanol oxidation

Catalyst oxide	Redox		Acidic	
	E_{app} (kcal/mol)	A_o (μmol/m^2 s)	E_{app} (kcal/mol)	A_o (μmol/m^2 s)
MgO	11	2.90E+03	–	–
CaO	20	6.50E+07	–	–
BaO	10	8.95E+03	–	–
Y$_2$O$_3$	6	1.45E+01	–	–
La$_2$O$_3$	10	2.41E+03	–	–
TiO$_2$	29	3.70E+10	37	1.40E+14
ZrO$_2$	–	–	60	2.30E+22
HfO$_2$	–	–	35	1.00E+13
CeO$_2$	–	–	–	–
V$_2$O$_5$	19	2.40E+08	53	1.14E+26
Nb$_2$O$_5$	–	–	37	2.50E+14
Ta$_2$O$_5$	–	–	30	1.40E+11
Cr$_2$O$_3$	12	1.54E+04	–	–
MoO$_3$	–	–	24	5.10E+11
WO$_3$	–	–	29	4.34E+12
Mn$_2$O$_3$	8	2.01E+03	–	–
Fe$_2$O$_3$	8	8.50E+02	28	4.50E+11
Co$_3$O$_4$	14	2.60E+05	–	–
Rh$_2$O$_3$	9	2.40E+03	–	–
NiO	11	2.77E+04	–	–
PdO	9	3.61E+04	–	–
PtO	–	–	–	–
CuO	11	1.11E+05	–	–
Ag$_2$O	13	3.30E+06	–	–
Au$_2$O$_3$	–	–	–	–
ZnO	17	3.07E+06	–	–
Al$_2$O$_3$	–	–	22	8.25E+08
Ga$_2$O$_3$	–	–	25	3.3E+10
In$_2$O$_3$	19	2.43E+07	25	3.00E+08
SiO$_2$	–	–	11	3.70E+07
SnO$_2$	23	3.40E+09	74	3.3E+30
Bi$_2$O$_3$	10	4.40E+03	–	–

conversion changed from 0 to >10%. PtO, Au$_2$O$_3$, Ag$_2$O, PdO and Rh$_2$O$_3$ are active at temperature <125 °C. The alkali metal oxides MgO, CaO, SrO and BaO show initial activity in the range of around 175–225 °C. Most of the metal oxides yielding acidic products, WO$_3$, V$_2$O$_5$, Ga$_2$O$_3$ and MoO$_3$ are active in the range of 170–200 °C. La$_2$O$_3$ and SiO$_2$ were extremely inactive with SiO$_2$ reacting >300 °C.

Fe$_2$O$_3$, MoO$_3$, Ga$_2$O$_3$, WO$_3$ and V$_2$O$_5$ produced significant quantities of isopropyl ether along with propylene. Ether is formed by a bimolecular reaction on acidic sites of the metal oxide catalysts. Ru$_2$O$_3$ and SeO$_2$ were previously observed to volatilize and, thus, were not investigated [33].

The apparent activation energies vary significantly across the various metal oxides: 5 kcal/mol for Y$_2$O$_3$ to 25 kcal/mol for Fe$_2$O$_3$ towards redox product formation, acetone, and 21 kcal/mol on Al$_2$O$_3$ to 75 kcal/mol on SnO$_2$ towards acidic product formation. Determination of activation energies for CeO$_2$ was not possible due to rapid deactivation or, as in the case of SiO$_2$, due to the formation of cracking products. The E_{app} was determined from the slope of the oxidation activity at different temperatures for each of the oxides investigated. The curve fit had a R^2 of >0.9 for all cases and higher than 0.95 for many of the oxides.

The TOFs were calculated by dividing the extrapolated activity data to 200 °C by the total number

of active surface sites. Much of the previously published work in isopropanol reaction literature is at 200 °C [11,17,18,34]. The TOFs towards redox products are seen to vary over six-orders of magnitude. PtO is the most active ($10^2 \, \text{s}^{-1}$) and TiO_2 the least active ($10^{-4} \, \text{s}^{-1}$). TOFs of acidic catalysts vary over eight-orders of magnitude.

3.4. TOF correlations

The isopropanol oxidation TOFs to acetone are plotted against the bulk heat of formation of the metal oxide normalized per oxygen atom in Fig. 1. The heats of formation were obtained from [35,33]. There is a correlation for the TOF redox with ΔH_f. At low ΔH_f values, the lower the heat of metal oxide formation, the more active the metal oxide catalyst. However, for intermediate and higher ΔH_f values, the TOFs are essentially constant. The redox TOFs versus the T_{onset} of TPR–H_2 is plotted in Fig. 2 and there does not appear to be any trend. The TOF versus the surface isopropoxide decomposition temperature

plot in Fig. 3 reveals a weak trend in the case of the redox TOFs. At low T_d values (<150 °C) the TOFs (redox) decreases with increasing decomposition temperature of the surface isopropoxide intermediates. However, for moderate (175–275 °C) and high T_d values (>300 °C) the TOFs (redox) is essentially constant. Redox selectivities are plotted against the corresponding TOFs, in Fig. 4. The selectivity was found to be independent of the TOFs for redox sites. The plot of $\ln(A_o)$ versus E_{app} for redox as well as acidic sites is almost a straight line, Figs. 5 and 6. Precious metal oxides, Au_2O_3 and PtO have not been included in the graphs. The very active and the very inactive oxides tend to deviate from the straight line.

4. Discussion

4.1. In situ Raman studies

The above results reveal the qualitative and quantitative nature of the pure metal oxide surfaces towards
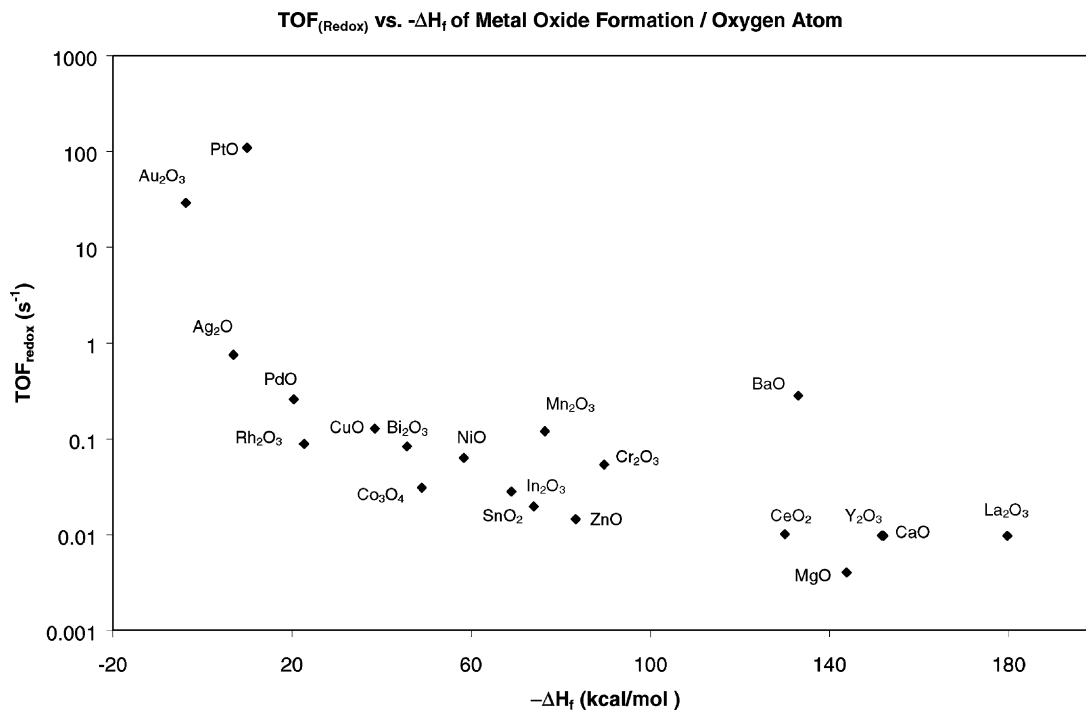

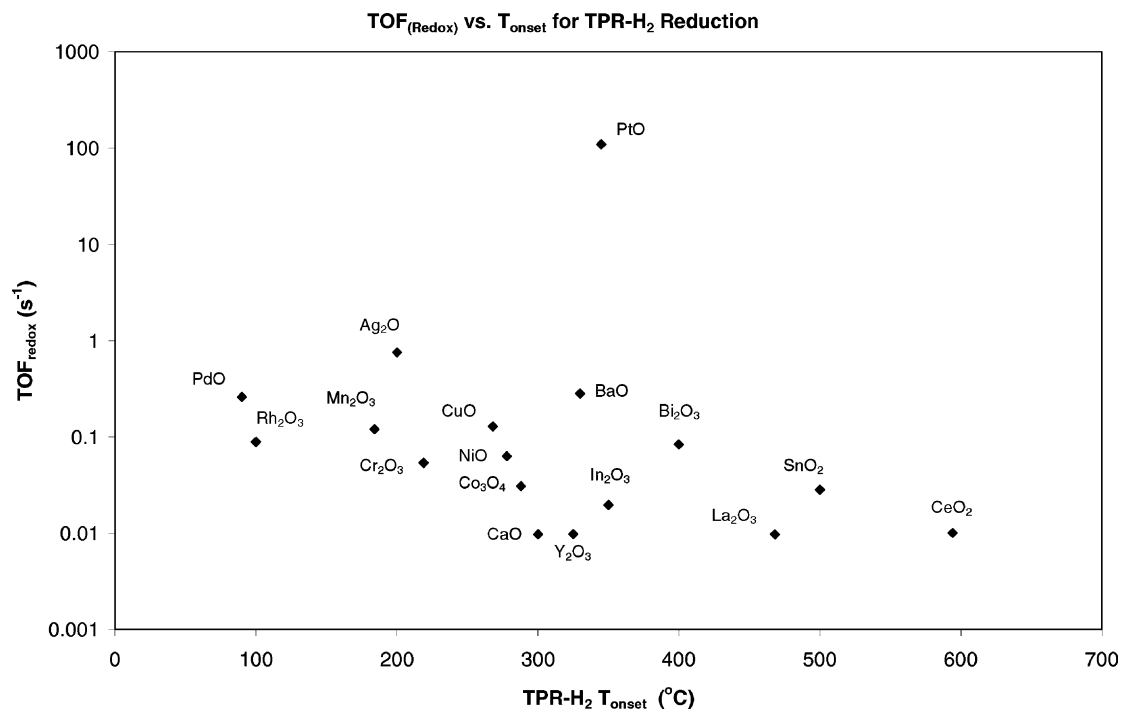Fig. 1. Semi-log plot of TOF$_{redox}$ vs. heat of formation of bulk oxide catalysts.

TOF$_{(Redox)}$ vs. T$_{onset}$ for TPR-H$_2$ Reduction

Fig. 2. Semi-log plot of TOF$_{redox}$ vs. T_{onset} TPR–H$_2$ reduction of bulk oxide catalysts.

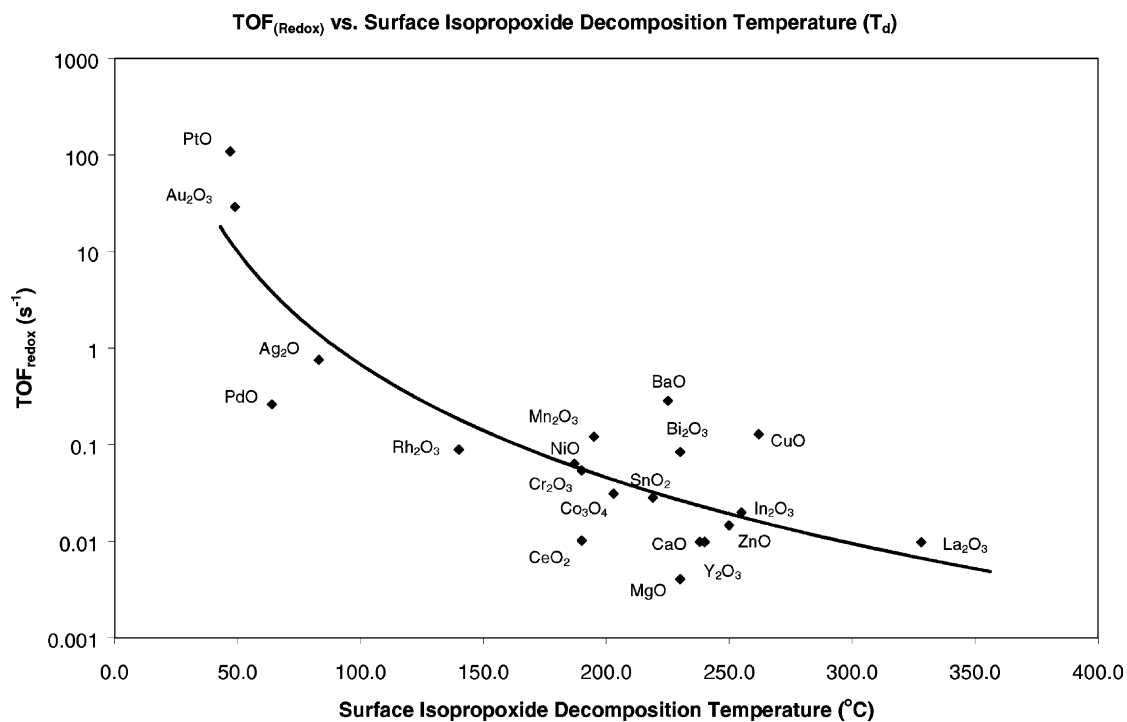**TOF$_{(Redox)}$ vs. Surface Isopropoxide Decomposition Temperature (T$_d$)**

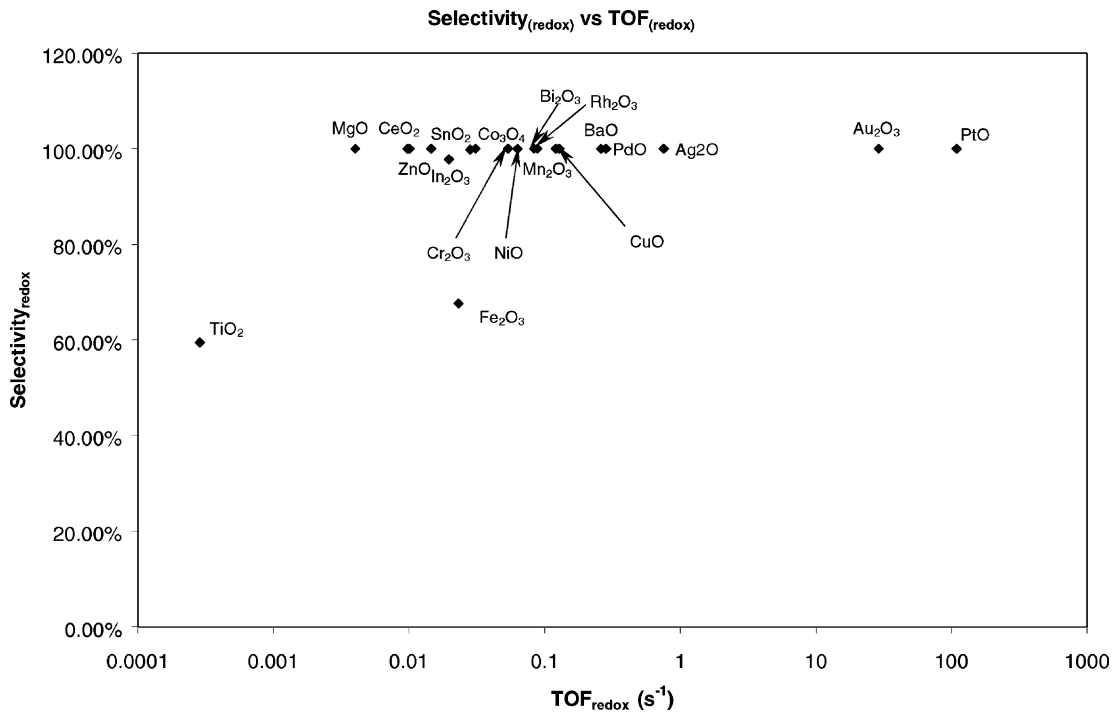Fig. 3. Semi-log plot of TOF$_{redox}$ vs. surface isopropoxide decompostion temperature.

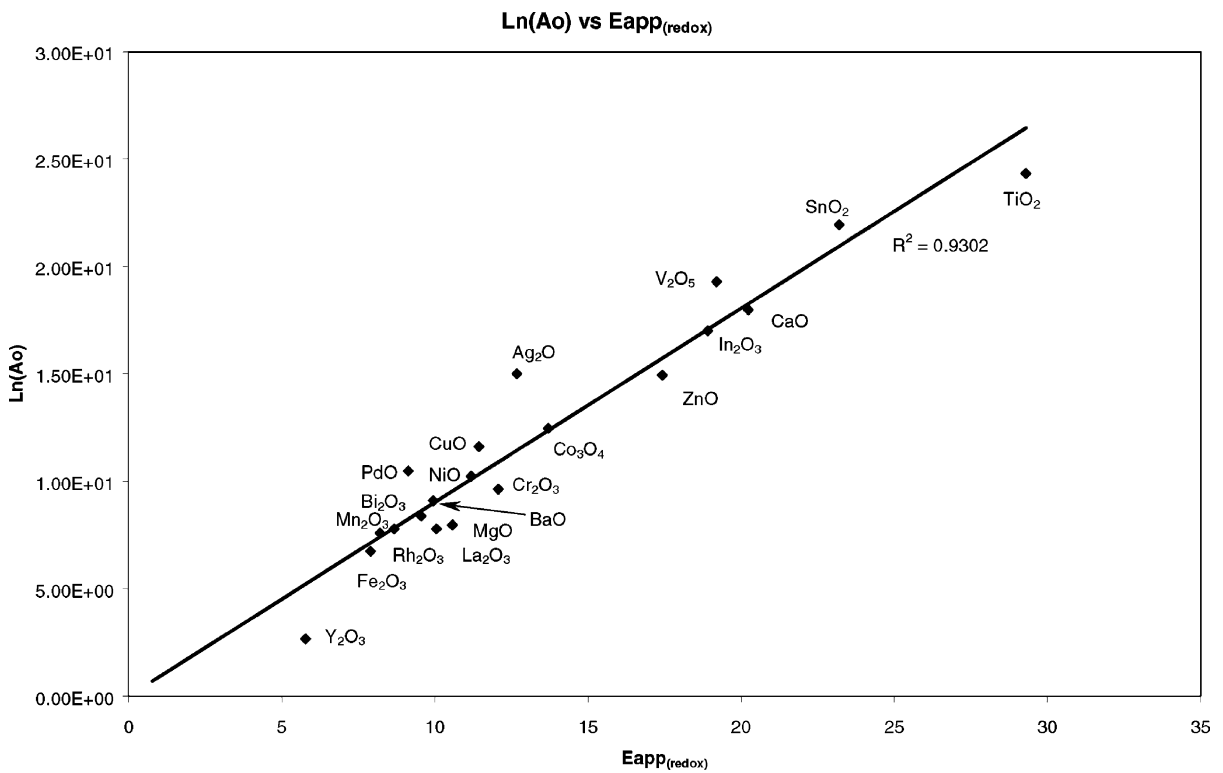Fig. 4. Plot of selectivity$_{redox}$ vs. semi-log TOF$_{redox}$.
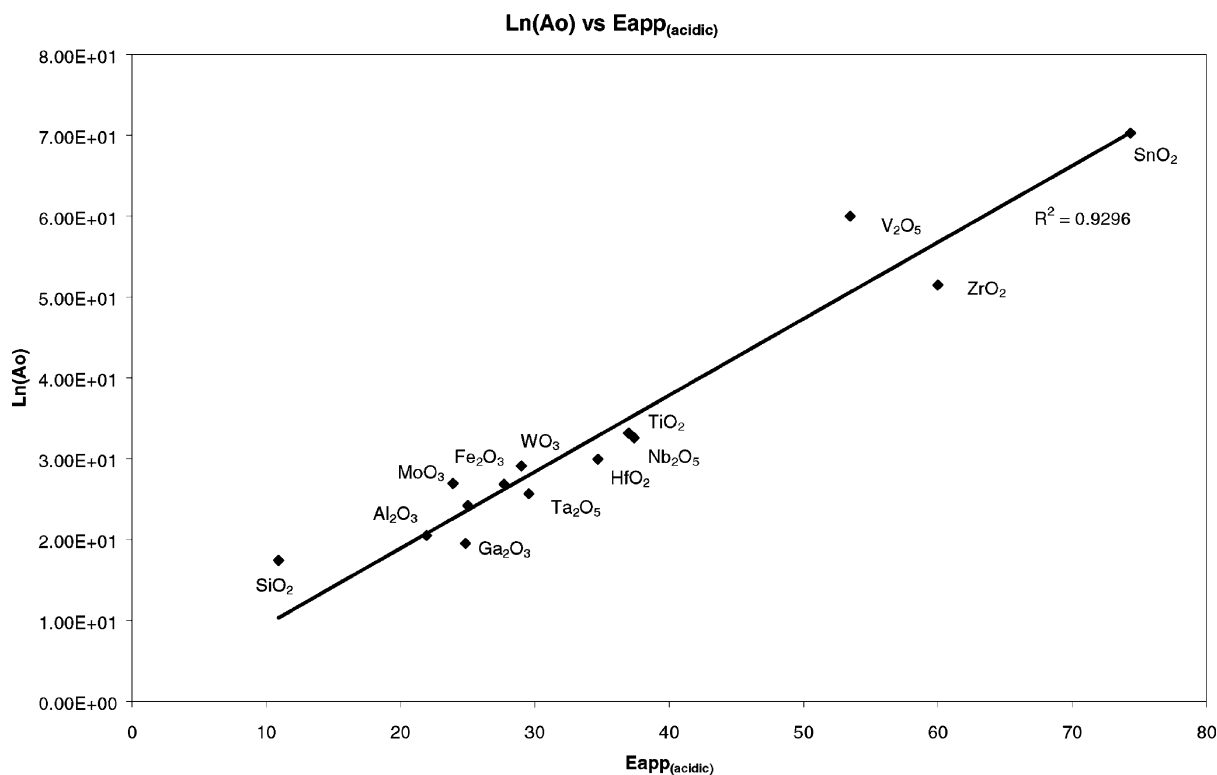

Fig. 5. Plot of $\ln(A_o)$ vs. $E_{app, redox}$.

Fig. 6. Plot of $\ln(A_o)$ vs. $E_{app,\,acidic}$.

isopropanol partial oxidation. Metal oxides with low values of bulk $-\Delta H_f$ (Rh_2O_3, PdO, PtO, Au_2O_3, Ag_2O and CuO), are suspected to undergo bulk reduction. However, previous methanol oxidation studies on Rh_2O_3, PdO and PtO with in situ Raman spectroscopy revealed that the surface of these metals remains oxidized under reaction conditions [36–38]. Similar results were obtained from in situ Raman spectroscopy studies during methanol oxidation on polycrystalline Ag [39–41] and X-ray absorption spectroscopy during methanol oxidation over Cu [40,41] where the surfaces were found to be Ag_2O and CuO, respectively. There are no such studies in literature on the oxidation state of Au_2O_3 during oxidation reactions. The unusually high number of surface sites on Au_2O_3, along with its extremely high activity and negative heat of formation suggests that there is some surface reduction of Au_2O_3. Isopropanol and methanol undergo a very similar surface reaction process, the OH group of the alcohol undergoes dissociative chemisorption

and subsequent breaking of the α-C–H bond results in the reaction products. Thus, it can be concluded that the other metal oxide surfaces remain essentially oxidized in the present study during isopropanol oxidation. Unlike the present study, where O_2 is in significant excess (13:2 ratio of O_2:$CH_3CHOHCH_3$), most of the previous studies were carried out with methanol in excess or with stoichometric amounts (1:1 ratio O_2:CH_3OH). This further supports the conclusion that excess O_2 ensures that the all other metal oxide surfaces remain completely oxidized under the present reaction conditions.

4.2. Number of active sites (N_s)

Quantifying the number of active surface sites on the metal oxide catalysts with isopropanol chemisorption is ideal for isopropanol oxidation since both chemisorption and oxidation proceed via the same surface isopropoxide intermediate. Furthermore, the

N_s values allow for the quantitative determination of the TOFs for isopropanol oxidation over the metal oxide catalysts. Cunnigham et al. [18], assumed an arbitrary value of one site for every $25\,(\text{Å})^2$, but pointed out the need for using an independent method for the determination of active surface site densities for the chemisorption of isopropanol on metal oxides than the conventional specific rates expressed per m^2. Upon converting the N_s value obtained in this study into active sites per unit area, an average value of one site per $\sim 50\,(\text{Å})^2$ is obtained. Expressing rates per m^2 neglects the intrinsic differences in the active surface site density of the catalysts. There is a variation of an order of magnitude between the active surface site densities on MgO ($8.9\,\mu\text{mol/m}^2$) and SiO$_2$ ($0.5\,\mu\text{mol/m}^2$), which are the extreme values. Au$_2$O$_3$($33\,\mu\text{mol/m}^2$) has uncommonly high number of active surface sites which can be attributed to the partial reduction of the oxide surface. Unless this difference is taken into consideration, there will be an error of an order of magnitude when comparing the TOFs between these two metal oxides.

Most of the catalysts in the present study possessed an active surface site density of around ~ 2–$4\,\mu\text{mol/m}^2$. SiO$_2$ had a low N_s value due to its extremely low surface activity. Some of the catalysts have extremely low surface areas and errors in their determination can cause a significant error in the determination of the active surface site density on these catalysts. The unusually low N_s value on BaO could be attributed to this factor. The low number of active surface sites on the Cr$_2$O$_3$ catalyst may be due to stearic interactions on the catalyst surface. There was no periodic trend observed across the columns or down the rows. In general, the precious metal oxides had a higher N_s value ($\sim 5.5\,\mu\text{mol/m}^2$). The N_s values for isopropanol adsorption were smaller than the N_s values previously obtained for methanol adsorption on MgO, La$_2$O$_3$, Cr$_2$O$_3$ [33]. Since similar catalytic samples were used in both studies and the same experimental set-up was used for the BET measurements, the decrease in N_s value can be attributed to the larger size of the isopropanol molecule. In the methanol chemisorption study, the high number of active surface sites observed for MgO, were attributed to the formation of surface carbonates [33]. The high value on MgO for isopropanol chemisorption could be due to a similar phenomenon. Very few values for N_s were found in literature. The value for TiO$_2$ from this study ($3.2\,\mu\text{mol/m}^2$) is comparable to the one found by Lusvardi et al. [16] ($6.1\,\mu\text{mol/m}^2$) and Carrizosa and Munuera [19,20] ($4.5\,\mu\text{mol/m}^2$). However, the number of surface sites observed on ZnO ($1.5\,\mu\text{mol/m}^2$) is somewhat lower than that reported by Koga et al. [25] ($6\,\mu\text{mol/m}^2$). The current active surface site measurement for MoO$_3$ ($1.2\,\mu\text{mol/m}^2$) closely matches the value of Farneth et al. [27] ($1.4\,\mu\text{mol/m}^2$). Farneth et al. also take into account the loss of one water molecule for every two isopropoxide species formed on the surface [27], which was demonstrated by using a molecular sieve to trap the desorbed water.

For supported metal oxide catalysts, the number surface metal oxide species are assumed to be the number of active sites, since they are completely dispersed on the surface of the oxide support [42]. For pure metal oxides and mixed bulk oxides, however, it is difficult to determine the number of active surface sites. On these oxides, it is necessary to determine the number of active surface sites with a molecule that can differentiate between the different sites and possesses similar stearic interactions upon adsorption as the actual reactant molecule. Measurements with CO, NH$_3$ and H$_2$/O$_2$ are inadequate since they are unable to distinguish between the nature of the various surface sites and possess different adsorption characteristics than the reactant molecule. Isopropanol undergoes surface reactions involving molecules with stearic interactions similar to the molecules involved in propane oxidation and could possibly be used as a probe molecule for determining the active surface sites for propane oxidation.

4.3. Isopropanol oxidation selectivities

Isopropanol oxidation yielded acetone, propylene and in some cases small amounts of isopropyl ether. By maintaining conversions <10%, heat and mass transfer limitations were minimized and the reaction was in the non-diffusional regime [15]. The product distribution under these conditions reflects the specific nature of the active surface sites since it minimizes secondary reactions. Low conversions minimize the complete oxidation of isopropanol on precious metal oxides. There has been some dispute in the literature about the reaction mechanism for propylene formation. Several researchers have proposed the oxidation

of bridge bonded surface isopropoxide species [14], while others have suggested coordinatively bonded and undissociated surface isopropanol for dehydration [24,28]. In either case, there is an oxygen interaction and, hence, there is an oxidation reaction. Most of the alkali metal oxides MgO, CaO, SrO and BaO yield pure redox products. Y_2O_3, La_2O_3, CeO_2, Cr_2O_3, Mn_2O_3, Co_3O_4, Rh_2O_3, NiO, PdO, PtO, CuO, Ag_2O, Au_2O_3, ZnO and Bi_2O_3 primarily yield redox products. Well-known acidic catalysts like Al_2O_3, Nb_2O_5, HfO_2, Ta_2O_5, WO_3 and Ga_2O_3 exhibited only acidic products. Fe_2O_3 and TiO_2 exhibit both acidic and redox sites, and very small amounts of redox products were found for V_2O_5, SnO_2 and In_2O_3. SiO_2 showed very low reactivity and at high temperatures yielded a number of products due to cracking reactions. There was no trend seen in the nature of the surface sites, acidic or redox, on the metal oxide catalysts and their position in the periodic table.

The results of the present study on TiO_2 are slightly different than those reported by Rekoske and Barteau [11], who observed higher selectivity to acetone (99%) on TiO_2 (anatase) with the partial pressure of isopropanol at approximately half the partial pressure used in this study and the conversion kept constant at 1% and 548 K. However, they found the selectivity to vary drastically with the partial pressure of oxygen. Niobium yielded only propylene, which is in agreement with observations by Ouqour et al. [15]. Cr_2O_3 and La_2O_3 yielded only acetone, which is in agreement with the published results of Gervasini and Auroux [34]. Most metal oxides that yielded basic and redox products with methanol oxidation (BaO, Cr_2O_3, Mn_2O_3, Co_3O_4 and Rh_2O_3) [33]; yielded only redox products with isopropanol oxidation. The acidic catalysts were previously found to be 100% selective for methanol oxidation [33] and similar results were found in the present study. V_2O_5 showed ~100% selectivity to acidic products in the present study, while for methanol oxidation it showed ~90% redox activity. Thus, each specific probe molecule possesses different sensitivity to acidic and redox surface sites.

4.4. TOFs for isopropanol oxidation

The TOFs on precious metal oxide catalysts are order of magnitudes higher PtO ($10^2\,s^{-1}$) and Au_2O_3

($10^1\,s^{-1}$) when compared to the TOFs of alkaline metal oxides MgO ($10^{-3}\,s^{-1}$). There is also a large variation between acidic TOFs with V_2O_5 ($10^1\,s^{-1}$) being the most active compared to ZrO_2 ($10^{-7}\,s^{-1}$) which is extremely inactive. There are very few TOF values for isopropanol oxidation published in the literature. The TOF values for acetone and propylene formation on TiO_2 obtained in this study, 2.9×10^{-4} and $2 \times 10^{-4}\,s^{-1}$, respectively, are in agreement with the values reported in the literature 1.8×10^{-5} to 1.5×10^{-3} and $8.2 \times 10^{-4}\,s^{-1}$ [11,18,34]. The TOF values were calculated by dividing the activity of TiO_2 at 200 °C in the various studies on TiO_2 with the N_s obtained by Lusvardi et al. [16] for TiO_2.

In the present experimental studies, it was not possible to quantitatively determine the individual contributions of the surface redox sites and acidic sites. However, the effect of the selectivity on the TOFs would be expected to be negligible, since the TOFs vary by four- to five-orders of magnitude and most of the selectivities approached 100%. Furthermore, most of the metal oxide catalysts studied, were either purely acidic or purely redox in nature, and hence, did not involve selectivity considerations. It was previously mentioned that there are possible errors in the measurement of N_s due to the inaccuracy in measuring the BET values of low surface area oxides. However, these uncertainties do no affect the calculation of the TOF values because activities and N_s are both expressed per m^2 and the possible corresponding errors in BET value cancel out.

Most of the previous studies focused on decomposition of isopropanol on metal oxide catalysts in the absence of gas phase O_2. Rekoske and Barteau [11] studied the effect oxygen on the partial oxidation of isopropanol on titania. According to their investigation, the major effect of the addition of O_2 is the prevention of surface reduction. In addition, the presence of O_2 completely inhibits H_2 formation, leads to hydroxyl as well as H_2O formation and oxidizes surface carbonaceous residue. In transient studies of photocatalytic oxidation of isopropanol on titania, Larson et al. [13] found that in excess of 1% oxygen the reaction is zero-order with respect to the oxygen partial pressure. In FTIR oxidation studies of isopropanol on Co_3O_4 by Finocchio et al. [14], it was concluded that the oxygen involved in the selective and non-selective oxidation of isopropanol is the "nucheophilic" lattice

oxygen. Thus, the isopropanol oxidation mechanism follows the Mars–van-Krevelen mechanism.

The dehydration reaction on Nb_2O_5 studied by Ouqour et al. [15] was found to follow Langmuir–Hinshelwood kinetics

$$r_p = k_p \lambda_i P_i / (1 + \lambda_i P_i) \qquad (4)$$

where r_p is the reaction rate, k_p the rate constant, λ_i the isopropanol equilibrium adsorption constant and P_i the partial pressure of isopropanol in the reactant stream. It was found that the reaction became zero-order with respect to isopropanol concentration >2 kPa. The operating partial pressure in the present study is a little in excess of 2 kPa. They also conclude that the surface reaction step involving α-C–H bond scission is the rate-determining step. Citing a number of studies, Gervasini and Auroux [34] also make the assumption that the isopropanol reaction is zero-order with respect to the isopropanol and oxygen partial pressures. This is in disagreement with Rekoske and Barteau [11] who suggested that reaction rate to acetone and propylene is one-half-order with respect to isopropanol partial pressure until partial pressures of 13.3 kPa. At sufficiently higher pressures, the surface becomes saturated and the reaction is zero-order with respect to the isopropanol partial pressure. However, unlike the present study, most of Barteau's work is performed under UHV on well-defined dehydroxlated metal oxide surfaces.

4.5. Apparent activation energy (E_{app})

The apparent activation energy values for isopropanol oxidation towards acetone are significantly lower than towards propylene. The E_{app} on metal oxides yielding only redox products was ~10 kcal/mol and is lower than the E_{app} to redox products for methanol oxidation (~20 kcal/mol) [43] because of the weaker C–H bond in the surface isopropoxide than in surface methoxide intermediate species. On oxides which yielded both redox and acidic products, $E_{app, redox}$ was ~8 kcal/mol for Fe_2O_3 and 29 kcal/mol for TiO_2. The E_{app} to acidic products varied over a wide range from 74 kcal/mol on SnO_2 to 22 kcal/mol on Al_2O_3. SiO_2 showed an uncommonly low E_{app} value towards propylene formation (11 kcal/mol), which is probably associated with the formation of multiple cracking products.

The apparent activation energy values and TOFs from various groups were compared with the values obtained in this study. Rekoske and Barteau [11] obtained a value of E_{app} of 17 kcal/mol for dehydrogenation and 31 kcal/mol for dehydration over TiO_2. In this study for TiO_2, the E_{app} values towards acetone and propylene formation were found to be 29 and 37 kcal/mol, respectively. These values compare well with other values for TiO_2 in literature (26 kcal/mol to redox products and 35 kcal/mol to acidic products) [17,18]. There does not seem to be a strong agreement between the E_{app} values obtained by Gervasini and Auroux [34] for all the oxides studied. This group used similar conditions except for the much higher contact times in the reactor.

4.6. Correlations

Plotting the TOFs versus various bulk parameters and surface parameters can provide a better fundamental understanding of the intrinsic dependence of the reaction. The plot of TOFs (redox) versus the bulk heat of formation of the metal oxides does show a weak trend (Fig. 1). For low bulk $-\Delta H_f$ values, the TOFs (redox) decrease rapidly and then decreases very slightly at higher $-\Delta H_f$ values. The lack of a strong trend for TOFs (redox) versus bulk $-\Delta H_f$ is not unexpected since the rate-determining step is the breaking of the α-C–H bond of the surface isopropoxide species to give acetone [15]. In the presence of oxygen there is little surface reduction and, hence, there are no limitations of oxygen diffusion from the bulk lattice. The reaction activity, which is a surface dependent phenomenon, is not inherently related to the bulk property of the metal oxide catalytic material.

Temperature programmed reduction (TPR) studies with H_2 indicate the ease of oxygen removal from the bulk metal oxide catalysts. Plotting the TOFs versus TPR–H_2 onset temperatures demonstrates that no correlation exists between these parameters. The onset reduction temperature of the metal oxide surface during TPR–H_2 can be limited by the rate of H_2 dissociation or by the rate of surface hydroxyl formation to H_2O, which may depend on the nature of the specific metal oxide. Plots of TOFs (redox) versus TPR–H_2 onset reduction temperatures (Fig. 2) reveal the unsuitability of correlating a surface property with a bulk property.

Unlike the reduction process, isopropanol undergoes dissociative adsorption on most catalyst surfaces, even at room temperature, to give surface isopropoxide and hydroxyl species [16,23,24,27]. The temperature at which these isopropoxide species can undergo further oxidation to give acetone or propylene determines the formation of products. It is suggested that for the dehydration reaction the bridge-bonded isopropoxide species are more stable and, hence, undergo oxidation at higher temperatures to lose a hydrogen atom [28], which leads to the formation of water along with propylene.

The plot of isopropanol oxidation TOFs (redox) versus the decomposition temperatures of the surface isopropoxide species (Fig. 3) shows a reasonable trend. A strong inverse trend is seen for very reactive surface isopropoxide species, but for less reactive surface isopropoxide species the decomposition temperature does not have a significant effect on the TOF of the oxide catalyst. Plot of isopropanol TOFs versus surface isopropoxide decomposition temperatures correlate two surface properties since both TOF and isopropoxide decomposition are surface parameters. This overcomes the limitations of comparing surface properties with bulk properties.

There have been few investigations into the relationship between reaction selectivity and activity across various metal oxide catalysts [34,17]. No trend is seen in Fig. 4 since most of the metal oxide catalysts exhibited a 100% selectivity to either acidic or redox products independent of the TOF, even though the TOFs varied by many orders of magnitude. There is a general belief in literature that extremely active metal oxides will lead to overoxidation. The present study shows contrary data. Thus, no correlation exists between the redox sites and the rate of reaction (TOF) on the surface sites for isopropanol oxidation.

As can be seen from Figs. 5 and 6, partial oxidation of isopropanol seems to show the compensation effect (type C—both E and A variable) as suggested by Boudart [44]. Inactive redox oxides like Y_2O_3 and extremely active oxides like Ag_2O tend to deviate from the general trend. Similarly acidic oxides like V_2O_5, which is very active and very inactive SiO_2 tend to drift away from the trend. Data from PtO and Au_2O_3 was not included in these figures since they are extremely active and hence have larger errors in determination of E_{app}.

5. Conclusions

Isopropanol chemisorption on the surface of various pure metal oxides at $110\,°C$ resulted in the formation of surface isopropoxide species. The surface species either underwent dehydrogenation or loss of a hydroxyl group to yield acetone or propylene, respectively. The number of active surface sites on the various pure metal oxides was $\sim$2–4 μmol/m^2. SiO_2, due to the unreactive nature of its surface, showed a much lower value for active surface site density and MgO exhibited a much higher value for active surface site density due to the formation of $MgCO_3$. Precious metals, had a slightly higher active surface site density. The selectivity of the various oxide catalysts to different products, under differential conversion conditions (<10% conversion), reflects the nature of the active surface sites, with redox sites yielding acetone and acidic sites yielding propylene. Surface isopropoxide species is the common reaction intermediate for isopropanol oxidation and isopropanol chemisorption. Thus, the number of chemisorbed surface isopropoxide species at $110\,°C$ was used to determine the TOF across the various metal oxide catalysts. The TOFs for acidic catalysts varied by eight-orders of magnitude (10^1 to $10^{-7}\,s^{-1}$) and TOFs for redox catalysts varied by six-orders of magnitude (10^2 to $10^{-4}\,s^{-1}$). There is a weak inverse correlation between the variation of the TOF (redox) and the bulk heats of formation of the metal oxides per oxygen atom at low $-\Delta H_f$. There is no correlation between TOFs and TPR–H$_2$ reduction onset temperatures. Variations of the TOFs (redox) with the surface isopropoxide intermediate decomposition temperatures reveal an inverse trend for the least stable surface intermediates and there is very little variation in TOFs (redox) with the decomposition temperature for the moderately and less reactive surface intermediates. The selectivity of the metal oxide catalysts is independent of the TOFs and is an inherent property of the nature of the active surface site.

References

[1] J.M. Thomas, W.J. Thomas, Principles of Heterogeneous Catalysis, VCH, New York, 1997.

[2] A.N. Desikan, L. Huang, S.T. Oyama, J. Phys. Chem. 95 (1991) 10050.

[3] K.V.R. Chary, V. Vijayakuma, P.K. Rao, Langmuir 6 (1990) 1549.

[4] B.M. Reddy, K.V.R. Chary, B.R. Rao, V.S. Subrahmanyam, C.S. Sunandana, N.K. Nag, Polyhedron 5 (1986) 191.

[5] F. Majunke, M. Baerns, A. Baiker, R.A. Koeppet, Catal. Today 20 (1994) 53.

[6] P.K. Rao, K. Narshimha, ACS Symp. Ser. 523 (1993) 231.

[7] K.V.R. Chary, J. Chem. Soc., Chem. Commun. (1989) 104.

[8] B.M. Reddy, B. Manohar, E.P. Reddy, Langmuir 9 (1993) 1781.

[9] K.V.R. Chary, B.R. Rao, V.S. Subrahmanyam, Appl. Catal. A: Gen. 74 (1991) 1.

[10] F. Arena, F. Frusteri, A. Paramliana, Appl. Catal. A: Gen. 176 (1999) 189.

[11] J.E. Rekoske, M.A. Barteau, J. Catal. 165 (1997) 57.

[12] M. Ai, S. Suzuki, J. Catal. 30 (1973) 362.

[13] S.A. Larson, J.A. Widegren, J. Falconer, J. L. Catal. 157 (1995) 611.

[14] E. Finocchio, R.J. Willey, G. Busca, V. Lorenzelli, J. Chem. Soc., Faraday Trans. 93 (1997) 175.

[15] A. Ouqour, G. Coudurier, J. Vedrine, J. Chem. Soc., Faraday. Trans. 89 (1993) 3151.

[16] V. Lusvardi, M. Barteau, W. Farneth, J. Catal. 153 (1995) 41.

[17] G.C. Bond, S. Flamerz, Appl. Catal. 33 (1987) 219.

[18] J. Cunningham, B.K. Hodnett, M. Ilyas, J. Tobin, E.L. Leahy, Faraday Discuss. Chem. Soc. 72 (1981) 283.

[19] I. Carrizosa, G. Munuera, J. Catal. 49 (1977) 174.

[20] I. Carrizosa, G. Munuera, J. Catal. 49 (1977) 189.

[21] A.I. Biaglow, R.J. Gorte, S. Srinivasan, A.K. Datye, Catal. Lett. 13 (1992) 313.

[22] J.E. Swain, M.V. Juskelis, J.P. Slanga, J.G. Miller, M. Uberio, N.D. Spencer, Appl. Catal. A: Gen. 139 (1996) 175.

[23] M.I. Zaki, G.A.M. Hussein, A.K.H. Nohman, Y.E. Nasheed, Thermochim. Acta 273 (1996) 257.

[24] M.I. Zaki, G.A.M. Hussein, H.A. El-Ammaay, S.A.A. Mansour, J. Polz, H. Knozinger, J. Mol. Catal. 57 (1990) 367.

[25] O. Koga, T. Onishi, K. Tamaru, J. Chem. Soc., Faraday Trans. 76 (1980) 19.

[26] J.M. Vohs, M.A. Barteau, J. Phys. Chem. 95 (1991) 297.

[27] W.E. Farneth, R.H. Staley, A.W. Sleight, J. Am. Chem. Soc. 108 (1986) 2327.

[28] G.A.M. Hussein, B.C. Gates, J. Catal. 176 (1998) 395.

[29] R. Groff, J. Catal. 84 (1984) 215.

[30] L. Braind, W. Farneth, I.E. Wachs, Catal. Today 62 (2000) 219.

[31] R.C. Weast (Ed.), Handbook of Chemistry and Physics, CRC Press, Boca Raton, 1986–1987.

[32] L.E. Briand, I.E. Wachs, J. Catal. 202 (2001) 268.

[33] M. Badlani, I.E. Wachs, Catal. Lett. 75 (2001) 137–149.

[34] A. Gervasini, A. Auroux, J. Catal. 131 (1991) 190.

[35] R.H. Perry, D.W. Green (Eds.), Perry's Chemical Engineering Handbook, Seventh Edition, McGraw-Hill, New York, 1997.

[36] C.T. Williams, C.G. Takoudis, M.J. Weaver, J. Phys. Chem. 102 (1998) 406.

[37] C.T. Williams, H.Y.H. Chan, A.A. Tolia, M.J. Weaver, C.G. Takoudis, Ind. Eng. Chem. Res. 37 (1998) 2307.

[38] H.Y.H. Chan, C.T. Williams, M.J. Weaver, C.G. Takoudis, J. Catal. 174 (1998) 191.

[39] C.B. Wang, G. Deo, I.E. Wachs, J. Phys. Chem. 103 (1999) 5645.

[40] A. Knop-Gericke, M. Havecker, T. Schedel-Niedrig, R. Schlogl, Catal. Lett. 66 (2000) 215.

[41] H. Werner, D. Herein, G. Schulz, U. Wild, R. Schlogl, Catal. Lett. 49 (1997) 109.

[42] G. Deo, I.E. Wachs, J. Haber, Crit. Rev. Surf. Chem. 4 (1994) 141.

[43] J.M. Tatibouet, Appl. Catal. A: Gen. 148 (1997) 213.

[44] M. Boudart, Kinetics of Chemical Processes, Prentice-Hall, Engelwood Cliffs, NJ, 1968, pp. 194–198.